CrossMark

Microbial Sorption of Uranium Using *Amycolatopsis* sp. K47 Isolated from Uranium Deposits

Fatih Celik · Mustafa Camas · Kwaku Kyeremeh · Anil Sazak Camas

Abstract The increasing contamination of soils, sediments, and water with heavy metals through natural and industrial processes is a worldwide problem. Mining processes produce tons of material contaminated with radionuclides such as U and different heavy metals such as Cd, Ni, and Pb. U(VI) adsorbs strongly on bacteria, exhibiting pH-dependent adsorption behavior that is caused by a range of uranyl surface complexes on bacteria cell walls. The *Amycolatopsis* sp. K47 was isolated from Manisa Koprubasi Kasar open-cast uranium mine and identified for the first time. Using the batch adsorption method, the biosorption potential of this microbe was investigated by studying the effects of changes in pH (1–10), biomass dose (0.1–5 g/l), initial uranium metal concentration (5–200 mg/l), contact time (5–180 min), and temperature (20–60 °C). Interpretation of FTIR data obtained for both the uranium loaded and unloaded *Amycolatopsis* sp. K47 biomass showed the presence of carboxylic acid, hydroxyl, and amide functional groups that could interact with uranium ions. Scanning electron microscopy images demonstrated that uranium was intensely adsorbed on the microbial biomass surface. The sorption isotherms were investigated by analysis of the Langmuir, Freundlich, and Dubinin–Radushkevich (D–R) models. The Langmuir isotherm model was found to show the best fit for the experimental data obtained. Furthermore, thermodynamic parameters, such as $\Delta H°$, $\Delta S°$, and $\Delta G°$, were calculated using adsorption equilibrium constant obtained from the Langmuir isotherm. The optimal experimental conditions were determined to be pH = 4, C_0 = 40 ppm, t = 150 min, temp. = 40 °C, and abs. dose = 1 g/l, and the corresponding U(VI) removal efficiency was about $97 \pm 2\%$.

1 Introduction

Uranium pollution is a global problem even though this element is considered as very rare in nature. Incidentally, there are hundreds of minerals in the earth's crust that contain uranium. Uranium is found worldwide in similar quantities as molybdenum and arsenic, but in higher quantities compared to silver, mercury, antimony, and cadmium. Furthermore, uranium is found in soils and rocks and also in natural water bodies. In the soil, uranium concentrations range between 1 and 5 mg/kg, while its concentrations in water are about 0.1–5 μg/l (Fetter and Von Hippel 1999; Payne 2010). Natural uranium is commonly found as U-238 (~97.3%), U-235 (~0.7%), and U-234 (~0.0054%) which is a degradation product of U-238, but several different

F. Celik (✉) · M. Camas · A. Sazak Camas
Department of Bioengineering, Munzur University,
62000 Tunceli, Turkey
e-mail: fatihcelik.dr@gmail.com

K. Kyeremeh
Department of Chemistry, School of Physical and Mathematical Sciences, University of Ghana, P.O. Box LG 56, Legon-Accra, Ghana

🙂 Springer

isotopes can be found in the earth's crust with a half-life of about three million years. It is the long half-life of uranium that makes its chemotoxic property more prominent compared to its radiotoxic property (Payne 2010). Uranium mining causes its release into the environment with physical and chemically processed mining waste containing uranium in amounts higher than internationally permitted levels (Xiaozhi Zhang et al. 1997). This element can reach the top of the food chain due to its long half-life and if ingested by humans and animals can cause serious harm to the body by accumulating in organs such as the lungs and kidneys (Bleise et al. 2002). Previous studies have shown that inhalation of diluted uranium can also cause very serious health hazards (Parrish et al. 2008). Exposure to uranium or its decay products even at low concentrations in the natural environment causes chemical and toxic effects similar to those of other non-radioactive heavy metals.

Removal of uranium and other toxic metals from water is possible with several chemical (e.g., neutralization and precipitation) and physical (e.g., evaporation, ion exchange, and membrane technology) methods. However, these methods require high capital investment and setup cost, but they are ineffective in low-resistance waters. Therefore, researchers have focused on finding easy, effective, economic, and environmentally friendly techniques to remove uranium and other heavy metals from aqueous solutions (Xiaozhi Zhang et al. 1997; Dushenkov et al. 1997; Aytas et al. 2015; Silva et al. 2009).

In recent years, thorough studies have been conducted on the use of plants (Dushenkov et al. 1997), algae (Aytas et al. 2015), seaweed (Silva et al. 2009), fungi (Yang et al. 2012; Abd El Hameeda et al. 2015), bacteria (Tsuruta 2003, 2006, 2011), yeast (Riordan et al. 1997), and similar biological materials to remove metal pollutants from aqueous solutions. Most importantly, the use of microbial biomass as an alternative method of removal or recycling natural pollutants, industrial waste, metal pollutants from materials used for military or civilian purposes, and radioactive or toxic heavy metals produced by mining has gained a lot of research interests. The results of these studies have shown that both the economic benefits and sorption capacity of these materials are high.

An excellent example of microbial biosorbents with high adsorption capacity that have been used for the biosorption of heavy metals is gram-positive bacteria. These bacteria are able to hold a wide variety of metal ions in their cell walls (Tsuruta 2003, 2006). The mechanism of biosorption has been found to involve electrostatic forces and Van der Waals interactions between the anionic carboxyl or phosphoryl groups present in the polymeric cellular walls of bacteria with metal ions. Metal adsorption is believed to occur in two stages: stoichiometric interaction between active chemical groups on the cellular wall and metals followed by accumulation of the metal on the biomass. Mayers and Beveridge conducted studies on the adsorption of different metal groups in water collected from lakes using *Bacillus subtilis* cellular walls in dilute aqueous solutions and found the results to be very encouraging (Mayers and Beveridge 1989). Currently, biosorbent bacteria have become commercially available for the removal of heavy metals from wastewater.

The genus *Amycolatopsis* belongs to the family *Pseudonocardiaceae* and includes 70 species with four subspecies (Embley et al. 1988). *Amycolatopsis* has attracted much attention as producers of bioactive compounds with biotechnological significance (Tang et al. 1998; Wink et al. 2003; Xu et al. 2003). Members of this genus are aerobic, gram- and catalase-positive, non-acid fast immobile actinomycetes that are meso-diaminopimelic in cellular wall peptidoglycan. They possess arabinose, galactose, and phosphatidylethanolamine as phospholipids, produce substrate mycelium (0.2–2 μm) but lack mycolic acids.

Herein, we present for the first time a study on uranium sorption conducted on a new *Amycolatopsis* sp. K47 (GenBank KT970733) which was identified by 16S rRNA gene sequence data after it was isolated and purified from soil samples collected from Manisa Koprubasi Kasar open-cast uranium mine. To the best of our knowledge, this report also represents the first successful study of uranium sorption capacity of an *Amycolatopsis* strain that was purified from a uranium mine. Batch adsorption method was used to investigate the effect of biomass quantity, initial metal concentration, solution temperature, and initial pH of the solution on microbial sorption.

2 Materials and Methods

2.1 Materials and Instrumentation

All the chemicals used were analytical grade, procured from Merck Corporation, and utilized in experiments

without any purification. Deionized ultrapure water (New Human Power-I Scholar UV, resistivity of 18.2 MΩ/cm, South Korea) was used for the preparation of solutions in all the experiments. Uranium stock solution with 1000 mg/l uranium metal (^{238}U) concentration was prepared with uranyl nitrate hexahydrate $UO_2(NO_3)_2 \cdot 6H_2O$ (Merck, Germany). pH adjustments of the solutions were conducted with 0.1 M ammonia and acetic acid solutions and a pH meter (Ezdo PL-700 PC, Taiwan). The pH value of solutions was measured before and after the reactions, and it was observed that the change was normally less than 0.1. However, measurement of pH changes during reactions was not possible. UV data measured on an Optima SP-3000 UV-VIS spectrophotometer was used to identify uranium. Functional groups were determined by Nicolet iS5 FTIR-ATR (Thermo Scientific, USA). Scanning electron microscope images were obtained from the JSM-6060 LV-SEM, while X-ray diffraction analysis was conducted by ARL K-Alpha (Thermo Scientific, USA).

2.2 Bacterial Isolation and Identification

The *Amycolatopsis* sp. K47 used in this study was isolated from soils obtained from Manisa Koprubasi Kasar region (Turkey) at 423-m altitude and 38.755801° N, 28.358597° E coordinates. The strain was isolated with ISP2 agar media supplemented with cycloheximide (50 μg/ml), nystatine (50 μg/ml), and nalidixic acid (25 μg/ml). The isolate K47 was purified in ISP2 agar media and maintained in 20% glycerol at − 20 °C. Genomic DNA of isolate was extracted with a DNA bacterial/fungal extraction kit according to the manufacturer's protocol (Zymo Research, USA). 16S rRNA gene was amplified by using universal bacterial 16S rRNA primers 27F and 1525R (Lane 1991). The PCR product was purified using a PCR purification kit, and direct sequence determination of the purified 16S rRNA gene was performed using universal sequencing primers 518F and 800R with an Applied Biosystems automated sequencer. Identification of the closest phylogenetic neighbors and calculation of pairwise 16S rRNA gene sequence similarities were achieved using the EzTaxon-e server (http://eztaxon-e.ezbiocloud.net) (Kim et al. 2012). The MEGA6 program was used for phylogenetic analysis, and the Clustal-W option in the same program was used for alignment (Tamura et al. 2013). Phylogenetic trees were inferred using

the neighbor-joining (Saitou and Nei 1987), maximum parsimony (Kluge and Farris 1969), and maximum likelihood (Felsenstein 1981) algorithms. Evolutionary distances were calculated using the Jukes and Cantor model. Topologies of the resultant trees were evaluated by bootstrap analysis (Felsenstein 1985) based on 1000 re-samplings.

2.3 Preparation of the Bacterial Biosorbent

The strain K47 was fermented in ISP2 broth for 5 days at 28 °C and centrifuged for 20 min at 4000 rpm; the obtained biomass was then lyophilized. Later on, the biomass which was dried for 24 h in an incubator (JSOF-50, JSR Model, Korea) at 70 °C was ground using a Tekmar A-10 model water-cooling mill. The powdered sample was sifted through a 250-μm (− 120 mesh) sieve, and the obtained lyophilized samples were stored at ambient temperature until used in biosorption experiments.

2.4 Biosorption Process

Batch adsorption method was conducted with a thermostatic shaker (WiseBath, WSB-30 Model). Experiments were carried out under the different conditions that are known to affect the adsorption process such as pH and initial concentration of the uranium solution, contact time, temperature, and amount of biomass used. For this procedure, 0.01 g lyophilized K47 was placed in a 15-ml polypropylene tube. The reaction was conducted by adding different concentrations (5–200 mg/l) of 10 ml $UO_2(NO_3)_2 \cdot 6H_2O$ solutions at 150 rpm shaking speed. This process was repeated for different times ranging between 5 and 180 min, different temperatures (20–60 °C), and pH (1–10). Sensitive and efficient determination of uranium was achieved by using Arsenazo III as a chromogenic reagent at pH 1.7 followed by spectrophotometric measurements. A stock Arsenazo III solution (1.0×10^{-4} mmol/ml) was prepared by dissolving the appropriate reagents. A universal buffer solution was prepared by adding drops of acetic acid, phosphoric acid, and boric acid sequentially until the final buffer pH was 1.7. The final pH of the buffer solution was measured with EZDO PL-700 PC model pH meter. The amount of uranium remaining in the solution after interaction with *Amycolatopsis* sp. K47 biomass was determined by spectrophotometric method.

In order to facilitate the spectrophotometric measurements, 2 ml of the universal buffer solution (pH 1.7), appropriate amounts (100 μl, for this study) of uranium adsorption mixture, and 2 ml of Arsenazo III solution (1.0×10^{-4} mmol/ml) were added to a 10-ml polypropylene tube and made up to the mark with triply distilled water. For each measurement, about 2 ml of the mixture solution was transferred to a spectrophotometric cell and absorbance was measured at 653 nm, against a reagent blank, for uranium ions. All measurements were performed three times and the mean values recorded (Niazi et al. 2007).

UO_2^{2+} amount adsorbed by *Amycolatopsis* sp. K47 was calculated using Eq. (1).

$$Q_e = (C_0 - C_e) \times \frac{V}{m} \qquad (1)$$

where Q_e depicts metal amount adsorbed per unit biosorbent (mg/g), C_0 and C_e depict pre-reaction and post-reaction UO_2^{2+} concentration in the solution, respectively (mg/l), V depicts the solution volume (l), and m depicts the biosorbent mass (g).

Metal ion distribution coefficient K_d (mg/l) between the aqueous and solid phases could be obtained with Eq. (2).

$$K_d = \left(\frac{C_0 - C_e}{C_e} \right) \times \frac{V}{m} \qquad (2)$$

where $\frac{V}{m}$ (ml/g) depicts the ratio of metal solution volume (ml) to biosorbent amount (g) in the batch adsorption process.

Percentage biosorption yield value was calculated using Eq. (3).

$$\%biosorption\ yield = \left(\frac{m_i - m_s}{m_i} \right) \times 100 \qquad (3)$$

In Eq. (3), m_i is the uranium amount loaded in the beginning (μg) and m_s is the uranium amount left in the solution after biosorption (μg).

2.5 Determination of *Amycolatopsis* sp. K47 Uranium(VI) Adsorption Capacity

Uranium adsorption capacity of the biomass was determined after optimal adsorption conditions were found. One hundred milligram *Amycolatopsis* sp. K47 samples were treated with pH 4.0, 10 ml 0.01 M $UO_2(NO_3)_2 \cdot 6H_2O$ solution in a shaker with

thermostat and water bath for 24 h at 40 °C and 150 rpm. After the solid and liquid phases were separated, the uranium amount left in the solution after adsorption was determined spectrophotometrically with the Arsenazo III method. Adsorbed uranium was calculated by difference between the initial and final or equilibrium concentrations of uranium. These measurements enabled the calculation of the adsorption capacity (Q_e, mg/g) of *Amycolatopsis* sp. K47.

3 Results and Discussion

3.1 Isolation and Identification

The *Amycolatopsis* sp. K47 used in the present study was isolated and purified successfully in ISP2 agar medium. In order to identify the K47 strain, sequenced data were aligned and its phylogenetic position with the closest relatives was identified. Thus, K47 strain forms a phyletic line within *Amycolatopsis* species and demonstrates 98.9% sequence similarity with its closest species type *A. rhabdoformis* SB026[T] in the neighbor-joining phylogenetic tree (Fig. 1).

3.2 Fourier-Transform Infrared Spectroscopy

FTIR spectroscopy was used to determine the functional groups in the ground *Amycolatopsis* sp. K47 strain. Measurements were taken on an IR spectrophotometer between 600 and 4000-cm^{-1} wavenumbers. The spectra in Fig. 2 shows (a) functional groups detected after interaction between ground K47 and uranium and (b) functional groups originally present in the ground K47.

In the IR spectrum of the unloaded K47, the very strong absorption band around 3200–3400 cm^{-1} was assigned to an O–H stretching of carboxylic acids due to the very pronounced broadening that almost threatens to overlap the peaks at 2937, 2925, and 2852 cm^{-1}. The presence of aliphatic (–CH and –CH$_2$) groups, amines, and amides with polymeric associations was inferred from the peaks at 2937, 2925, and 2852 cm^{-1}. Higher frequency absorption around 1630 cm^{-1} is called the amide I band. The lower frequency amide II band around 1530 ± 30 cm^{-1} is largely due to N–H bending trans to the carbonyl oxygen (Li et al. 2008). The absorption
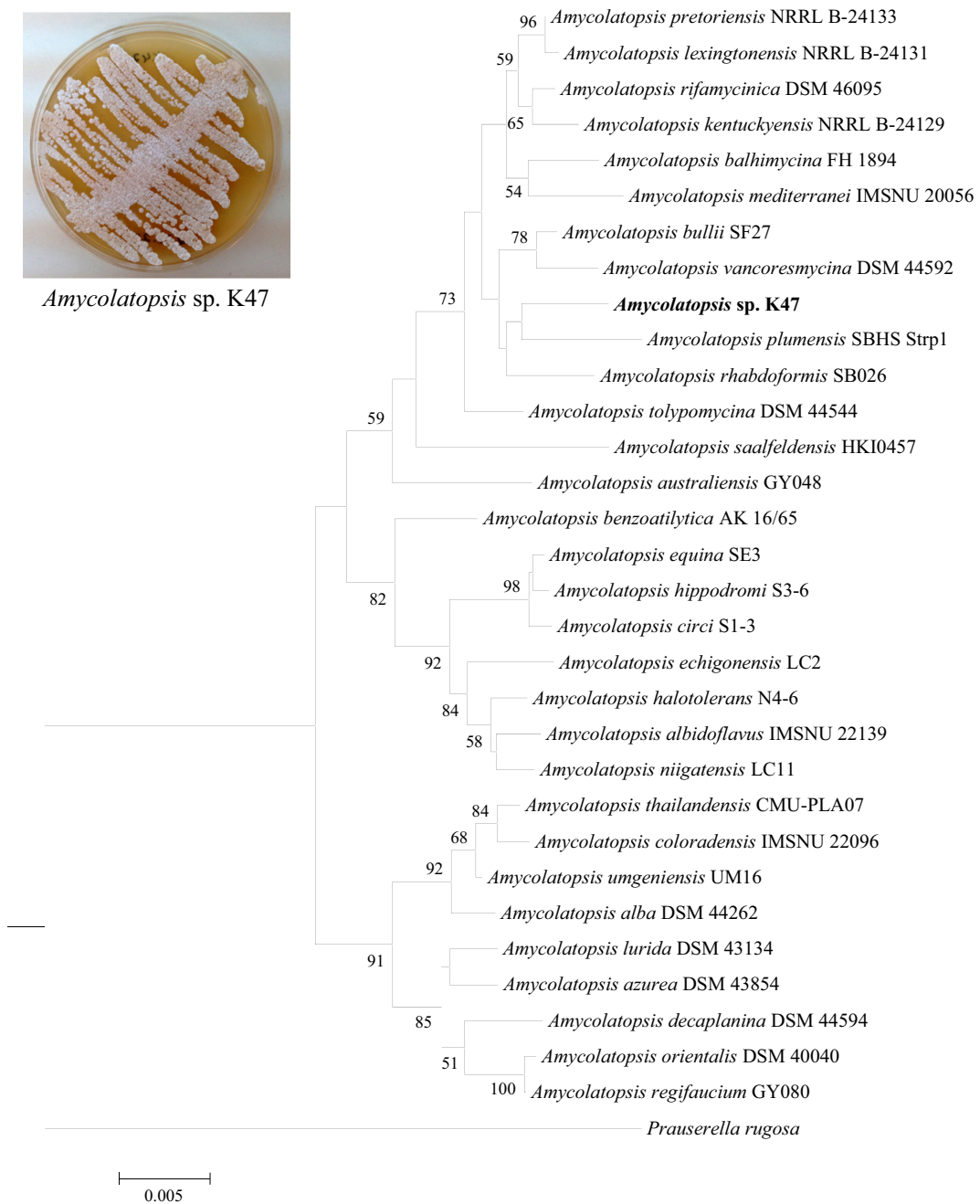
Amycolatopsis sp. K47

Fig. 1 Phylogenetic tree based on 16S rRNA gene sequences showing the relationships of strain K47 and related taxa. The dendrogram was reconstructed by using the neighbor-joining method. Bootstrap values (based on 1000 replicates) greater than 50% are shown at nodes. Bar, 0.005 sequence dissimilarity per nucleotide position. GenBank KT970733

bands at 1450–1394 and 1230 cm^{-1} were assigned to characteristic C–O–H bending and C–O stretching vibrations, respectively, which further confirms the presence of COOH groups or derivatives that could be involved in metal biosorption (Yee et al. 2004). C–

N and C–O functional group stretching bands overlapped at around 1000–1020 cm^{-1}.

In the spectrum of loaded K47, no significant differences were observed except for the peak at 913-cm^{-1} wavenumber. The presence of this new peak in loaded
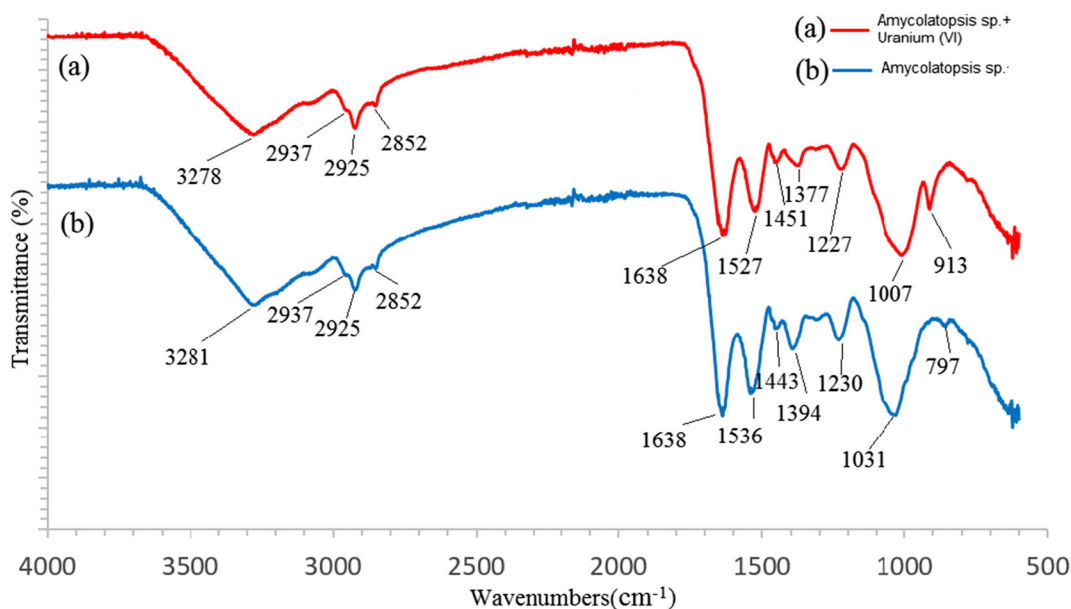
Fig. 2 Infrared spectra of **a** loaded and **b** unloaded Amycolatopsis sp. K47 biomass

biomass was attributed to heavy metal ion–oxygen bond (Chhikara et al. 2010). Hence, it was concluded that *Amycolatopsis* sp. K47 cell surfaces have abundant carboxylic acid, hydroxyl, and amide groups. Biosorption is most likely to occur as a result of ionic interactions between uranium ions and functional groups associated with the polysaccharides and proteins in the cell walls of *Amycolatopsis* sp. K47 (Volesky 1990).

3.3 Scanning Electron Microscopy

SEM was used to determine the physical properties of the microbial biosorbent material including particle shapes, surface morphology, surface texture, and adequate size distribution. The changes in surface structure for uranium loaded and unloaded *Amycolatopsis* sp. K47 biosorbent were observed by illumination with ×5000 and ×20,000 magnifications as shown in Fig. 3. The images show a high level porous and irregular biomass surface which enables a high rate of uranium adsorption (Aytas et al. 2015). In SEM images, dense metals are seen in light gray and white colors, while the amorphous structures are seen in dark colors (Gunther et al. 2008; Lloyd et al. 2009). The gray brightness that occurs after the interaction with uranium shows the presence of the metal. Therefore, the SEM images

demonstrated that uranium was intensely adsorbed on the biomass surface.

3.4 Examining Uranium Adsorption Conditions

3.4.1 Effect of pH on Uranium Adsorption to Biosorbent

Previous studies on heavy metal adsorption has demonstrated that pH is a significant parameter that affects biosorption since it is responsible for the ionization of biosorbent surface functional groups and adsorption of metal ions on the surface (Gok and Aytas 2009). Based on the measurements conducted using 10 mg biosorbent at 30 °C for 2 h and with 100 mg/l constant uranium concentration between pH 1 and 10, the graph that shows the correlation between the percentage uranium adsorption by the biosorbent and equilibrium constant (K_d) is presented in Fig. 4a. Consequently, when all other parameters remain constant under the abovementioned conditions, maximum bioadsorption yield occurs around pH 4 (88.3%, K_d 7328 ml/g). Hence, around pH 4, there could be various hydrolyzed oligomeric and monomeric forms of UO_2^{2+}. The relative ratios of these types are determined by the total uranium concentration in the environment and the effect of pH (Hu et al. 1996). It is important to note that there is competition between the adsorption of H_3O^+ and UO_2^{+2} ions between pH 1 and 4. In aqueous
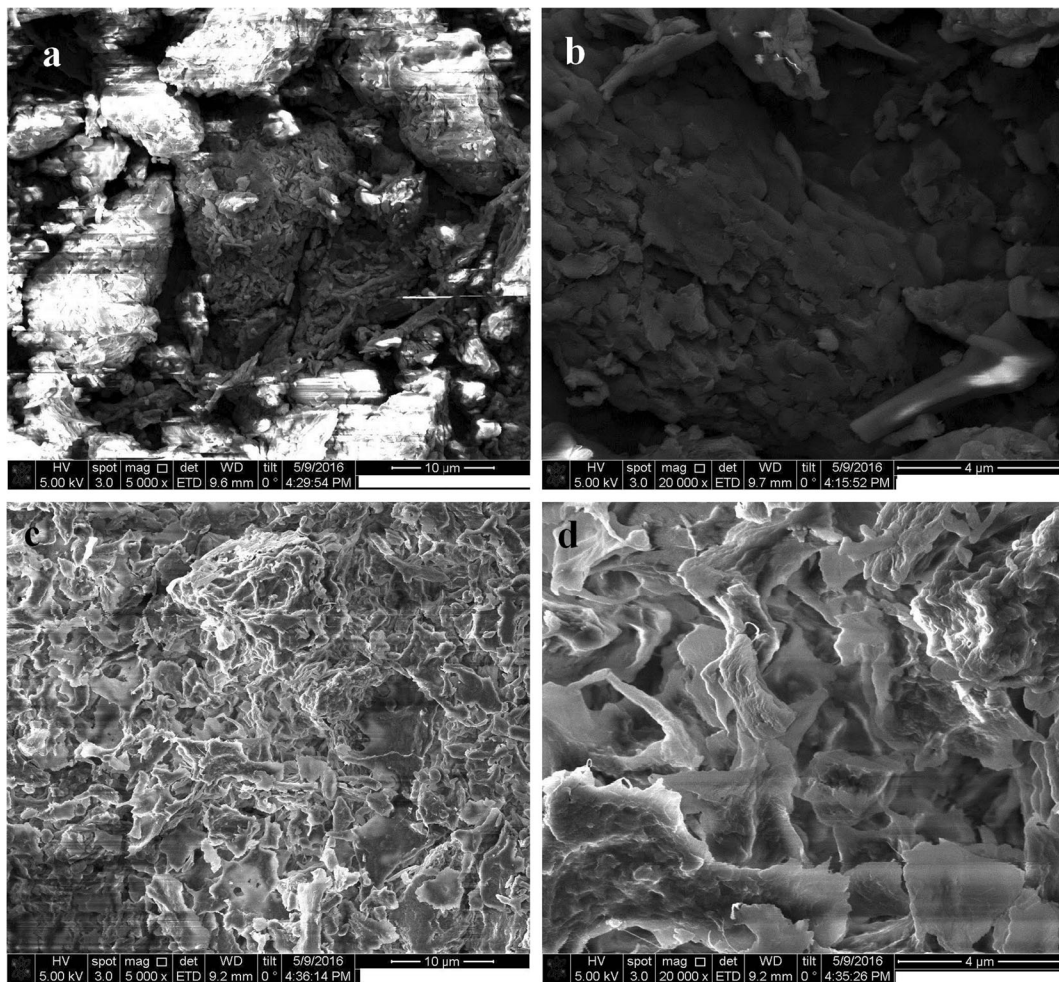
Fig. 3 Scanning micrographs of Amycolatopsis sp. K47 biosorbent at **a** ×5000 and **b** ×20,000. The Amycolatopsis sp. K47 biosorbent which has come into contact with uranium at **c** ×5000 and **d** ×20,000

solutions, uranyl ions are quite stable at pH < 2.5, but at pH 4, UO_2^{+2} is the predominant species in solution. At this pH, UO_2OH^+ ions are found at the rate of 2.2% and their maximum value reaches 18.6% at pH 6. $UO_2(OH)_2$ percentage at pH 4 was calculated as 1.5%, and after pH 8, its maximum value was 99.4% (Fig. 4b) (Li et al. 2016). Around pH 7, uranyl ions form strong complexes with carbonates, but above this pH, many of these ions could not be detected due to precipitation as a result of hydroxide ion formation. Therefore, between pH 7 and 10, $UO_2(CO_3)_2^{2-}$ and $UO_2(CO_3)_3^{4-}$ anion types, which are soluble carbonate complexes of UO_2^{2+}, are dominant. At pH < 10, the amount of $UO_2(OH)_3^-$ ions present in solution is negligible. Above pH 10 in carbonate-free water, hydroxide complexes are formed as $(UO_2)_2(OH)_2^{2+}$, UO_2OH^+, and $(UO_2)_3(OH)_5^+$ (Sorg 1991; Qadeer and Saleem 1997).

3.4.2 Effect of Microbial Biosorbent Dose

To investigate the effects of biosorbent dose, uranium solutions were prepared at pH 4, in 10-ml polypropylene tubes with uranium concentration of 100 mg/l. These solutions were exposed to 0.1–10 g/l amounts of *Amycolatopsis* sp. K47 biomass at 30 °C temperature for 2 h. It was observed that biosorbent dosage was effective on sorption, and the findings are presented in Fig. 5. As a result of these tests, the most active biosorption yield was found as 87.7% (K_d 7153 ml/g) for 1 g/l dose of biomass.
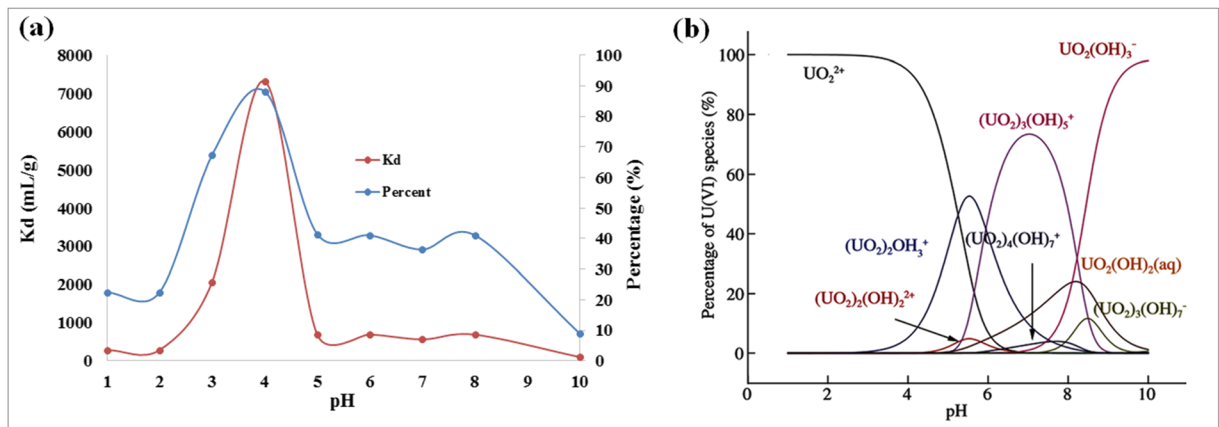
Fig. 4 Effect of pH on **a** U(VI) biosorption by Amycolatopsis sp. K47 and **b** speciation of U(VI) in solution. Adsorption conditions: $C_0 =$ 40.0 mg/l, V 10 ml, m 0.01 g, $T = 30$ °C, and contact time 2 h

As the biosorbent dose increased, sorption yield decreased considerably. This situation could have occurred due to the decrease in surface area as a result of the aggregation of the biomass at high biosorbent dosage (Gok et al. 2013).

3.4.3 Effect of Uranium(VI) Concentration

Biosorption yield of uranium(VI) with *Amycolatopsis* sp. K47 biomass was examined in solutions with 5–200 mg/l initial concentrations, temperature adjust at 30 °C, pH 4, biomass dose 1 g/l, and the contact time of 2 h. Under

these conditions, biosorption yield increased until 40 mg/l U(VI) concentration; it reached the maximum yield at 40 mg/l (86.3%, K_d 6067 ml/g), and after this value, biosorption yield decreased since the areas where the uranium ions would be adsorbed became saturated. The results of these experiments are as shown in Fig. 6.

3.4.4 Effect of Contact Time on the Adsorption Process

Mixing time is an active parameter of adsorption. In uranium adsorption on *Amycolatopsis* sp. K47 biosorbent, the effect of interaction time was studied
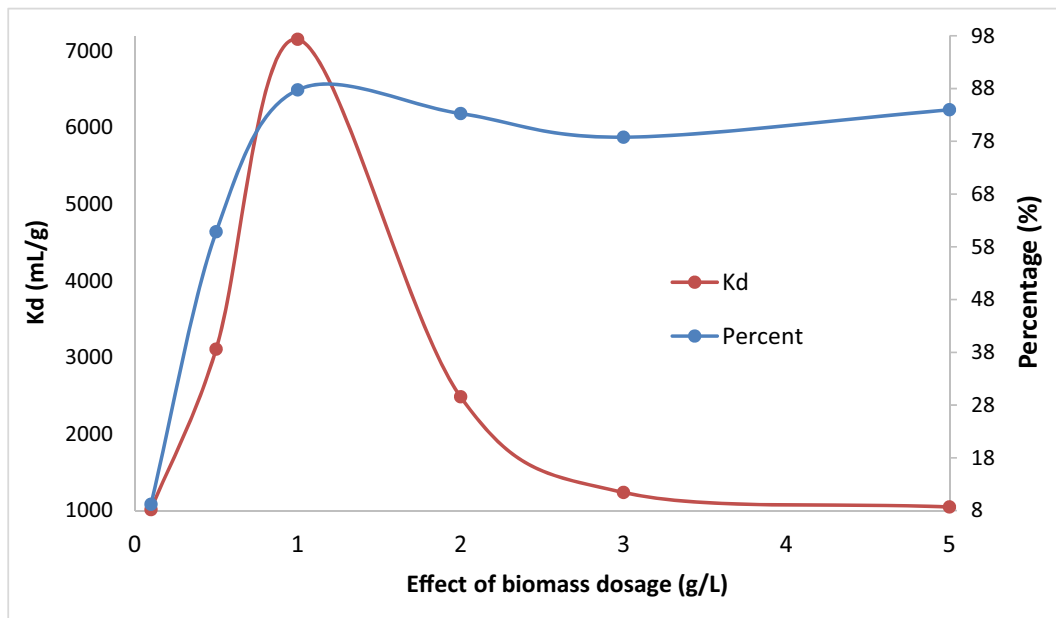

Fig. 5 Effect of biomass dose in adsorption of uranium on Amycolatopsis sp. K47 (pH 4, initial U(VI) concentration 40 mg/l, V 10 ml, temp. 40 °C, contact time 2 h)
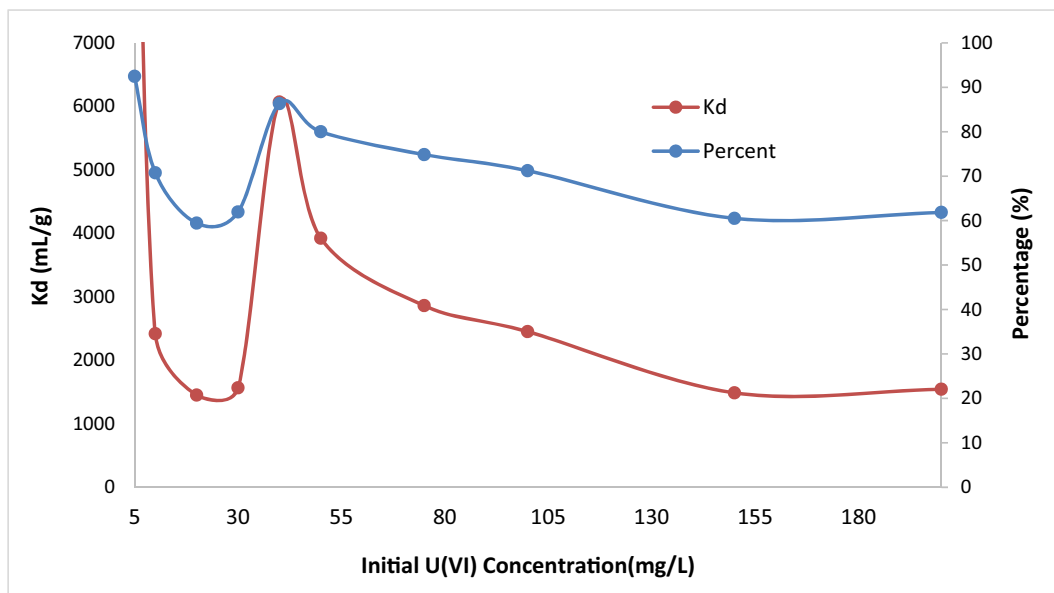
Fig. 6 The effect of initial concentration on the adsorption of uranium on Amycolatopsis sp. K47 (pH 4, time 2 h, *V* 10 ml, *m* 0.01 g, *T* 30 °C)

within the 10–180-min timeframe. The change in uranium adsorption from the solution on biomass and distribution coefficient based on the change in contact time is shown in Fig. 7.

While uranium interaction at the end of 15 min was 45.5%, the distribution coefficient K_d was 835 ml/g for *Amycolatopsis* sp. K47 biosorbent. At the end of 180-min shaking period, it was observed that uranium adsorption yield increased by 61% and K_d increased until 1569.7 ml/g. Considering that the applied process was economic and equilibrium was obtained at the end of 150-min mixing period, adsorption yield was found to be 66.2% and K_d 1907.8 ml/g. Therefore, this duration was accepted as the optimal mixing period.

3.4.5 Effect of Temperature on the Adsorption Process

Temperature of the biosorption environment is important for all energy-dependent mechanisms. The possibility of energy-independent mechanisms to be affected by the changes in ambient temperature is considerably lower (Gok et al. 2010). To investigate the effect of the ambient temperature on the adsorption of uranium by the biosorbent, 0.01 g *Amycolatopsis* sp. K47 biomass was shaken at pH 4 with 20, 30, 40, 50, and 60 °C temperatures for 120 min in a water bath with a thermostat. The results obtained are presented in Fig. 8. The data showed that while adsorption yield of uranium ion

at 20 °C was 82% and distribution coefficient was 4489, as the temperature was raised to 40 °C, adsorption yield rose to 94% and K_d decreased to 4000, but when the temperature was increased to 60 °C, adsorption yield of uranium ion dropped to 64% with K_d decreasing to 1772. The optimum operational temperature was determined as 40 °C. The decrease in biosorption yield with increase in temperature could be due to the decrease in absorptive power in adjacent molecules of the adsorbed phase and active groups for sorption between the biosorban/biosorbent (Yusan et al. 2010).

3.5 Isotherm Calculations

To determine the adsorption capacity of the biosorbent, equilibrium data were assessed based on Freundlich, Langmuir, and Dubinin–Radushkevich (D–R) isotherms. These isotherm equations are the most commonly used isotherms in determination of the adsorption equilibrium in water and wastewater applications (Yusan and Akyil 2008). The Langmuir Eq. (4) which has been applied to several biosorption processes successfully is given below.

$$\frac{C_e}{Q_e} = \frac{1}{bn_m} + \frac{C_e}{n_m} \qquad (4)$$

In this equation, C_e is equilibrium concentration (mg/l), Q_e is adsorbed substance amount per unit
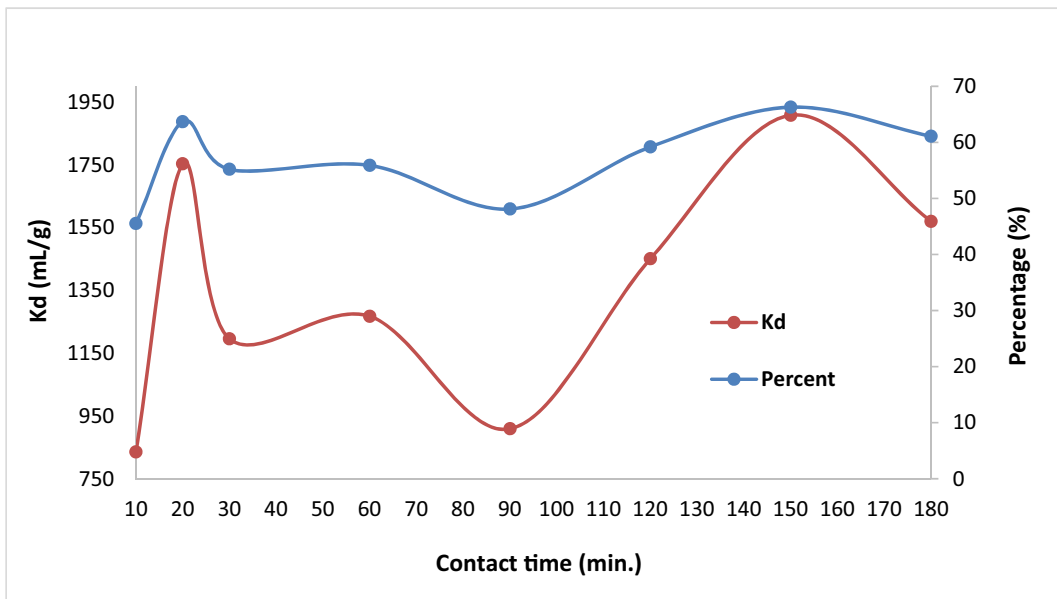
Fig. 7 The effect of contact time on the adsorption of uranium on Amycolatopsis sp. K47 (pH 4, initial U(VI) cons 40 mg/l, *V* 10 ml, *m* 0.01 g, *T* 30 °C)

mass at equilibrium (mg/g), and n_m and b are Langmuir constants related to single layer sorption capacity (mg/g) and sorption energy (l/mg), respectively. Langmuir isotherm indicates that the adsorption surface is single layer. This model is based on the hypothesis that adsorbent is structurally homogenous and all adsorption regions on the surface are the same with respect to energy (Kutahyali and Eral 2010). Freundlich isotherm Eq. (5) provides information on the biosorption
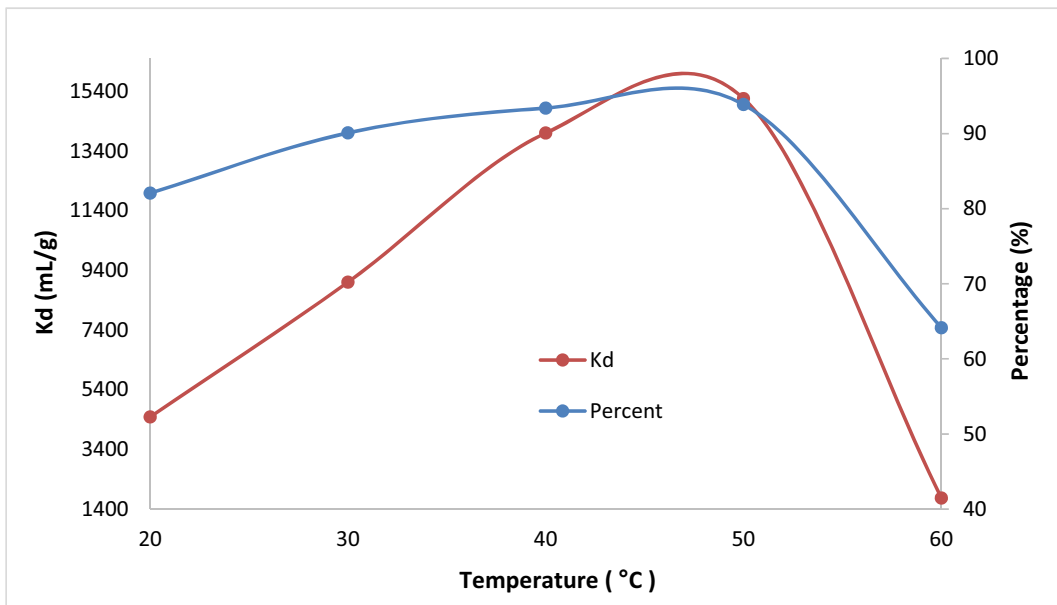

Fig. 8 Effect of temperature on the adsorption of uranium on Amycolatopsis sp. K47 (pH 4, initial U(VI) cons 40 mg/l, *V* 10 ml, *m* 0.01 g, contact time 150 min)

Table 1 Langmuir, Freundlich, and D–R constants for the adsorption of U(VI) on *Amycolatopsis* sp. K47

Langmuir isotherm			Freundlich isotherm			Dubinin–Radushkevich (D–R) isotherm			
R^2	n_m (mg/g)	b (l/mg)	R^2	n (l/mg)	K_F (mg/g)	R^2	K (mol^2/kJ^2)	X_m (mol/g)	EDR (kJ/mol)
0.9881	2500	0.8	0.9171	0.9171	75.12	0.9497	0.0000104	0.22	218.72

of U(VI) on a biosorbent with a heterogeneous surface.

$$Q_e = K_F \times C_e^{1/n} \qquad (5)$$

When Eq. (5) is reorganized into a linear form (Eq. 6), the following equation is obtained:

$$log Q_e = log K_F + \frac{1}{n} log C_e \qquad (6)$$

In this equation, Q_e represents the adsorbed substance per unit biosorbent mass (mg/g), C_e represents equilibrium concentration of the solution (mg/l), and K_F and n are the characteristic constants of the Freundlich isotherm. These constants are identified by the slope n of the graph plotted between Q_e and C_e, and its intersection point K_F.

D–R adsorption isotherm is defined as the energy released during the adsorption of 1 mol ion from the solution by the adsorbent. D–R adsorption isotherms are used to calculate adsorption energy. Adsorption energy is found by the slope of these isotherms. At the same time, D–R isotherm model

could be used to define the adsorption on homogeneous and heterogeneous surfaces under low concentration ranges. It assumes adsorption in regions close to the surface. D–R adsorption Eq. (7) is expressed as follows:

$$ln X = ln X_m - K\varepsilon^2 \qquad (7)$$

In the equation, $ln X$ depicts the Polanyi potential and is calculated by solving the Eq. (8).

$$\varepsilon = RT \left(1 + \frac{1}{C_e} \right) \qquad (8)$$

In these equations, X is the adsorbed substance per unit adsorbent mass (mg/g), X_m is the theoretical adsorption capacity (mmol/g), C_e is the metal concentration at equilibrium (mg/l), K is the constant dependent on the adsorption energy, R is the general gas constant, and T is the temperature in Kelvin. A linear graph can be plotted between X and ε^2. The values are found by the slope (K) and intersection (X_m). Mean sorption energy (E) is the free energy exchange that occurs during the transfer of
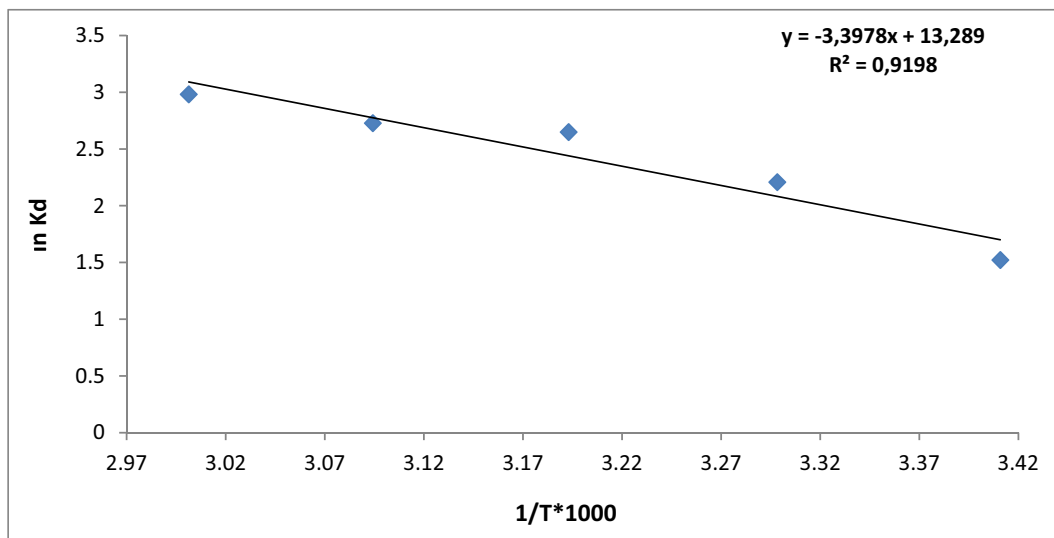

Fig. 9 ln K_d and $1/T$ curve for U(VI) adsorption on Amycolatopsis sp. K47 (pH 4, U(VI) concentration 40 mg/l, contact time 150 min, V 10 ml, and m 0.01 g)

Table 2 Thermodynamic parameters for U(VI) bioadsorption on the *Amycolatopsis* sp. K47

	$\Delta H°$ (kJ/mol)	$\Delta S°$ (kJ/mol K)	$\Delta G°$ (kJ/mol)				
			298 K	303 K	308 K	313 K	323 K
Amycolatopsis sp. K47	−22.57	−0.14	18.55	19.96	21.37	22.77	24.17

1 mol of the solid in the solution onto the surface and can be calculated with Eq. (9).

$$E = -(2K)^{-1/2} \qquad (9)$$

E value is used to estimate the mechanism of the reaction. If E value is between 8 and 16 kJ/mol, ion exchange mechanism is active. If $E < 8$ kJ/mol, physical forces could affect the reaction mechanism. When $E > 16$ kJ/mol, particle diffusion is predominant in the sorption. Freundlich, Langmuir, and D–R isotherm data are presented in Table 1.

When adsorption models were examined, it could be observed that the most suitable model was Langmuir isotherm model ($R^2 = 0.9881$). Furthermore, the fact that EDR (kJ/mol) > 16 demonstrated that particle population was more dominant in this sorption study. Since Freundlich isotherm constant ($n = 0.9171$) was $0 < n < 10$, it was deduced that positive adsorption conditions were obtained.

3.6 Thermodynamic Calculations

To determine the thermodynamic parameters ($\Delta H°$, $\Delta S°$, and $\Delta G°$) of U(VI) adsorption onto *Amycolatopsis* sp. K47, biosorption processes were conducted under optimum conditions with the main parameters pH, contact time, biosorbent dose, and initial U(VI) concentration with temperatures ranging between 20 and 65 °C.

Adsorption enthalpy was calculated using the method based on the Van't Hoff plot. The values of $\Delta H°$ and $\Delta S°$ were calculated from the slopes and intercepts of the linear variation of $\ln K_d$. Thermodynamic stability constant with reciprocal of temperature $1/T$ (Fig. 9) was calculated using the relation (10) below (Sert and Eral 2010).

$$lnK_d = \frac{\Delta S^0}{R} - \frac{\Delta H^0}{RT} \qquad (10)$$

In Eq. 10, $\Delta H^0 \left(\frac{kj}{mol}\right)$ and $\Delta S^0 \left(\frac{j}{mol.K}\right)$ depict standard enthalpy and standard entropy changes, respectively, R

depicts the ideal gas constant ($8.314 \frac{J}{mol\,K}$), and T depicts absolute temperature (K).

In a specific adsorption process, standard Gibbs energy is calculated by the equation (ΔG^0):

$$\Delta G^0 = \Delta H^0 - T\Delta S^0 \qquad (11)$$

Thermodynamic parameters obtained for U(VI) biosorption are given in Table 2.

The fact that $\Delta G > 0$ at the point of equilibrium for the measurements conducted under optimum conditions of Gibbs free energy exchange demonstrates that the reaction no longer proceed towards the products by itself but rather proceed towards the inputs. Generally, free energy exchange is between −20 and 0 kJ/mol in physicosorption and between −80 and −400 in chemisorption. Negative enthalpy exchange −22.57 kJ/mol shows that there is a physical sorption that includes weak affinity, and at the same time, the sorption is exothermic. This shows that sorption process has stable energy. Negative entropy exchange corresponds to the decrease in the degree of freedom of adsorbed types (Kavak 2009).

4 Conclusion

Purified *Amycolatopsis* sp. K47 mycelia was dried, ground, and filtered through a 250-μm sieve. FTIR spectroscopy confirmed the presence of carboxylic acids, hydroxyls, and amide functional groups that could be responsible for the intense adsorption of uranium ions on the microbial biomass surface. SEM surface analysis confirmed the surface morphology and physical properties of the biosorbent. The images obtained were very characteristic of a biomass surface which is highly porous and irregular and allows highly intense adsorption of uranium ions.

The optimum uranium adsorption conditions were pH 4, biomass dose 1 g/l, initial uranium(VI) concentration 40 mg/l, contact time 150 min, and temperature 40 °C. Under these conditions, maximum uranium

adsorption yield and K_d were calculated as $97 \pm 2\%$ and 3850 ml/g, respectively. The adequacy of the adsorption data obtained in 5–200 mg/l uranium concentration range and at constant temperatures to Langmuir, Freundlich, and D–R isotherms was investigated. The most adequate model was the Langmuir isotherm model ($R^2 = 0.9881$). Furthermore, the fact that EDR (kJ/mol) > 16 showed that particle population was more dominant in this adsorption study. The Freundlich isotherm constant ($n = 0.9171$) of $0 < n < 10$ demonstrated that positive adsorption conditions were fulfilled. For adsorption of uranium by *Amycolatopsis* sp. K47 biosorbent, adsorption enthalpy and entropy exchange values were found to be $\Delta H° - 22.50$ kJ/mol and $\Delta S° - 0.014$ kJ/mol K, respectively. It was shown that as the temperature increased, $\Delta G°$ reached higher values.

The findings of this study has shown that *Amycolatopsis* sp. K47 strain could be used with high yield in the adsorption/biosorption of uranium from dilute aqueous solutions. In the future, designed biosorbents based on this new strain could serve as a potential and alternative natural material in the removal of uranium in seawater and dilute aqueous solutions.

Furthermore, the present study could be extended in the future to the purification of biosorbents from different natural materials and their application to the removal of various radionuclides from our environment.

References

Abd El Hameeda, A. H., Wedad, E. E., Abou-Taleba, K. A. A., & Mirab, H. I. (2015). Biosorption of uranium and heavy metals using some local fungi isolated from phosphatic fertilizers. *Annals of Agricultural Sciences, 60*(2), 345–351. https://doi.org/10.1016/j.aoas.2015.10.003.

Aytas, S., Sezer, H., & Gok, C. (2015). Characterization of Cystoseira sp. for the isolation of uranium. *Analytical Letters, 49*(4), 523–540. https://doi.org/10.1080/00032719.2015.1076832.

Bleise, A., Danesi, P. R., & Burkart, W. (2002). Properties, use and health effects of depleted uranium (DU): a general overview. *Journal of Environmental Radioactivity, 64*, 93–112.

Chhikara, S., Hooda, A., Rana, L., & Dhankhar, R. (2010). Chromium (VI) biosorption by immobilized Aspergillus niger in continuous flow system with special reference to FTIR analysis. *Journal of Environmental Biology, 31*(5), 561–566.

Dushenkov, S., Vasudev, D., Kapulnik, Y., Gleba, D., Fleisher, D., Ting, K. C., et al. (1997). Removal of uranium from water using terrestrial plants. *Environmental Science Technology, 31*(12), 3468–3474. https://doi.org/10.1021/es970220l.

Embley, M. T., Smida, J., & Stackebrandt, E. (1988). The phylogeny of mycolate-less wall chemotype-iv actinomycetes and description of Pseudonocardiaceae Fam-Nov. *Systematic and Applied Microbiology, 11*(1), 44–52.

Felsenstein, J. (1981). Evolutionary trees from DNA sequences: a maximum likelihood approach. *Journal of Molecular Evolution, 17*(6), 368–376.

Felsenstein, J. (1985). Phylogenies and the comparative method. *The American Naturalist, 125*(1), 1–15.

Fetter, S., & Von Hippel, F. N. (1999). The hazard posed by depleted uranium munitions. *Science & Global Security, 1999, 8*(2), 125–161.

Gok, C., & Aytas, S. (2009). Biosorption of uranium(VI) from aqueous solution using calcium alginate beads. *Journal of Hazardous Materials, 168*(1), 369–375. https://doi.org/10.1016/j.jhazmat.2009.02.063.

Gok, C., Turkozu, D. A., & Aytas, S. (2010). Removal of Th(IV) ions from aqueous solution using bi-functionalized algae-yeast biosorbent. *Journal of Radioanalytical and Nuclear Chemistry, 287*(2), 533–541. https://doi.org/10.1007/s10967-010-0788-x.

Gok, C., Gerstmann, U., Hollriegl, V., & Aytas, S. (2013). Preparation of Ca-alginate biopolymer beads and investigation of their decorporation characteristics for 85Sr, 238U and 234Th by in vitro experiments. *Radiation Protection Dosimetry, 153*(1), 47–55. https://doi.org/10.1093/rpd/ncs088.

Gunther, A., Raff, J., Geipel, G., & Bernhard, G. (2008). Spectroscopic investigations of U(VI) species sorbed by the green algae Chlorella vulgaris. *Biometals, 21*(3), 333–341. https://doi.org/10.1007/s10534-007-9122-7.

Hu, M. Z., Norman, J. M., Faison, B. D., & Reeves, M. E. (1996). Biosorption of uranium by Pseudomonas aeruginosa strain CSU: characterization and comparison studies. *Biotechnology and Bioengineering, 51*(2), 237–247. https://doi.org/10.1002/(SICI)1097-0290(19960720)51:2<237::AID-BIT14>3.0.CO;2-J.

Kavak, D. (2009). Removal of boron from aqueous solutions by batch adsorption on calcined alunite using experimental design. *Journal of Hazardous Materials, 163*(1), 308–314. https://doi.org/10.1016/j.jhazmat.2008.06.093.

Kim, O. S., Cho, Y. J., Lee, K., Yoon, S. H., Kim, M., Na, H., et al. (2012). Introducing EzTaxon-e: a prokaryotic 16S rRNA gene sequence database with phylotypes that represent uncultured species. *International Journal of Systematic and Evolutionary Microbiology, 62*, 716–721. https://doi.org/10.1099/ijs.0.038075-0.

Kluge, A. G., & Farris, J. S. (1969). Quantitative phyletics and the evolution of anurans. *Systematic Zoology, 18*, 1–32.

Kutahyali, C., & Eral, M. (2010). Sorption studies of uranium and thorium on activated carbon prepared from olive stones: kinetic and thermodynamic aspects. *Journal of Nuclear Materials, 396*(1–2), 251–256.

Lane, D. J. (1991). *16S/23S rRNA sequencing. Nucleic acid techniques in bacterial systematics* (pp. 115–175). Chichester: John Wiley and Sons.

Li, H., Liu, T., Li, Z., & Deng, L. (2008). Low-cost supports used to immobilize fungi and reliable technique for removal hexavalent chromium in wastewater. *Bioresource Technology, 99*, 2234–2241.

Li, X., Ding, C., Liao, J., Du, L., Sun, Q., Yang, J., et al. (2016). Bioaccumulation characterization of uranium by a novel Streptomyces sporoverrucosus dwc-3. *Journal of Environmental Sciences (China), 41*, 162–171. https://doi.org/10.1016/j.jes.2015.06.007.

Lloyd, N. S., Mosselmans, J. F. W., Parrish, R. R., Chenery, S. R. N., Hainsworth, S. V., & Kemp, S. J. (2009). The morphologies and compositions of depleted uranium particles from an environmental case study. *Mineralogical Magazine, 73*(3), 495–510.

Mayers, I. T., & Beveridge, T. J. (1989). The sorption of metals to Bacillus subtilis walls from dilute solutions and simulated Hamilton Harbour (Lake Ontario) water. *Canadian Journal of Microbiology, 35*(8), 764–770. https://doi.org/10.1139/m89-128.

Niazi, A., Ghasemi, N., Goodarzi, M., & Ebadi, A. (2007). Simultaneous spectrophotometric determination of uranium and thorium using Arsenazo III by H-point standard addition method and partial least squares regression. *Journal of the Chinese Chemical Society, 54*(2), 411–418. https://doi.org/10.1002/jccs.200700058.

Parrish, R. R., Horstwood, M., Arnason, J. G., Chenery, S., Brewer, T., Lloyd, N. S., et al. (2008). Depleted uranium contamination by inhalation exposure and its detection after approximately 20 years: implications for human health assessment. *Science of the Total Environment, 390*(1), 58–68. https://doi.org/10.1016/j.scitotenv.2007.09.044.

Payne, T. E. (2010). Uranium. In D. A. Atwood (Ed.), *Radionuclides in the environment* (pp. 261–272). Chichester: John Wiley & Sons Ltd.

Qadeer, R., & Saleem, M. (1997). Adsorption of UO22+ ions on activated charcoal: pH effect. *Adsorption Science & Technology, 15*(5), 373–376. https://doi.org/10.1177/026361749701500505.

Riordan, C., Bustard, M., Putt, R., & McHale, A. P. (1997). Removal of uranium from solution using residual brewery yeast: combined biosorption and precipitation. *Biotechnology Letters, 19*(4), 385–387.

Saitou, N., & Nei, M. (1987). The neighbor-joining method: a new method for reconstructing phylogenetic trees. *Molecular Biology and Evolution, 4*(4), 406–425.

Sert, Ş., & Eral, M. (2010). Uranium adsorption studies on aminopropyl modified mesoporous sorbent (NH2–MCM-41) using statistical design method. *Journal of Nuclear Materials, 406*(3), 285–292. https://doi.org/10.1016/j.jnucmat.2010.08.024.

Silva, J. I. R., de Melo Ferreira, A. C., & da Costa, A. C. A. (2009). Uranium biosorption under dynamic conditions: Preliminary tests with Sargassum filipendula in real radioactive wastewater containing Ba, Cr, Fe, Mn, Pb, Ca and Mg. *Journal of Radioanalytical and Nuclear Chemistry, 279*(3), 909–914. https://doi.org/10.1007/s10967-008-7366-5.

Sorg, T. J. (1991). Removal of uranium from drinking water by conventional treatment methods. In C. A. Rebers (Ed.), *Radon, Radium and Uranium in Drinking Water* (pp. 173–191). Michigan: Lewis Publishers.

Tamura, K., Stecher, G., Peterson, D., Filipski, A., & Kumar, S. (2013). MEGA6: Molecular Evolutionary Genetics Analysis version 6.0. *Molecular Biology and Evolution, 30*(12), 2725–2729. https://doi.org/10.1093/molbev/mst197.

Tang, L., Yoon, Y. J., Choi, C. Y., & Hutchinson, C. R. (1998). Characterization of the enzymatic domains in the modular polyketide synthase involved in rifamycin B biosynthesis by Amycolatopsis mediterranei. *Gene, 216*(2), 255–265. https://doi.org/10.1016/S0378-1119(98)00338-2.

Tsuruta, T. (2003). Accumulation of uranyl and thorium by microorganism. *Journal General and Application Microbiology, 49*, 215–218.

Tsuruta, T. (2006). Accumulation of thorium and uranium by microbes—the effect of pH, concentration of metals, and time course on the accumulation of both elements using Streptomyces levoris. *Journal of Nuclear and Radiochemical Sciences, 7*, 1–6.

Tsuruta, T. (2011). Biosorption of uranium for environmental applications using bacteria isolated from the uranium deposits. In I. Ahmad, F. Ahmad, & J. Pichtel (Eds.), *Microbes and Microbial Technology* (pp. 267–281). New York: Springer.

Volesky, B. (1990). *Biosorption of heavy metals* (pp. 408). Boca Raton: CRC Press.

Wink, J. M., Kroppenstedt, R. M., Ganguli, B. N., Nadkarni, S. R., Schumann, P., Seibert, G., et al. (2003). Three new antibiotic producing species of the genus Amycolatopsis, Amycolatopsis balhimycina sp nov., A-tolypomycina sp nov., A-vancoresmycina sp nov., and description of Amycolatopsis keratiniphila subsp keratiniphila subsp nov and A-keratiniphila subsp nogabecina subsp nov. *Systematic and Applied Microbiology, 26*(1), 38–46. https://doi.org/10.1078/072320203322337290.

Xiaozhi Zhang, S. L., Yang, Q., Zhang, H., & Li, J. (1997). Accumulation of uranium at low concentration by the green alga Scenedesmus obliquus 34. *Journal of Applied Phycology, 9*, 65–71.

Xu, J., Mahmud, T., & Floss, H. G. (2003). Isolation and characterization of 27-O-demethylrifamycin SV methyltransferase provides new insights into the post-PKS modification steps during the biosynthesis of the antitubercular drug rifamycin B by Amycolatopsis mediterranei S699. *Archives of Biochemistry and Biophysics, 411*(2), 277–288. https://doi.org/10.1016/S0003-9861(03)0004-3.

Yang, H. B., Tan, N., Wu, F. J., Liu, H. J., Sun, M., She, Z. G., et al. (2012). Biosorption of uranium(VI) by a mangrove endophytic fungus Fusarium sp. #ZZF51 from the South China Sea. *Journal of Radioanalytical and Nuclear Chemistry, 292*(3), 1011–1016. https://doi.org/10.1007/s10967-011-1552-6.

Yee, N., Benning, L. G., Phoenix, V. R., & Ferris, F. G. (2004). Characterization of metalcyanobacteria sorption reactions: a combined macroscopic and infrared spectroscopic investigation. *Environmental Science & Technology, 38*, 775–782.

Yusan, S. D., & Akyil, S. (2008). Sorption of uranium(VI) from aqueous solutions by akaganeite. *Journal of Hazardous Materials, 160*(2–3), 388–395. https://doi.org/10.1016/j.jhazmat.2008.03.009.

Yusan, S., Aslani, M. A. A., Turkozu, D. A., Aycan, H. A., Aytas, S., & Akyil, S. (2010). Adsorptionand thermodynamic behaviour of U(VI) on the tendurek volcanic tuff. *Journal of Radioanalytical and Nuclear Chemistry, 283*(1), 231–238. https://doi.org/10.1007/s10967-009-0312-3.